

Statistical quality assessment of Ising-based annealer outputs

Krzysztof Domino ^{*1}, Mátyás Koniorczyk ^{†2}, and
Zbigniew Puchała^{1,3}

¹Institute of Theoretical and Applied Informatics, Polish Academy of Sciences, Bałycka 5, 44-100 Gliwice, Poland

²Wigner Research Centre, Budapest, Hungary

³Faculty of Physics, Astronomy and Applied Computer Science,
Jagiellonian University, 30-348 Kraków, Poland

December 8, 2021

Abstract

The ability to evaluate the outcomes of quantum annealers is essential for such devices to be used in complex computational tasks. We introduce a statistical test of the quality of Ising-based annealers' output based on the data only, assessing the ground state's probability of being sampled. A higher probability value implies that at least the lower part of the spectrum is a part of the sample. Assuming a plausible model of the univariate energy distribution of the sample, we express the ground-state energy and temperature as a function of cumulants up to the third order. Using the annealer samples, we evaluate this multiple times using Bootstrap resampling, resulting in an estimated histogram of ground-state energies, and deduce the desired parameter on this basis. The approach provides an easily implementable method for the primary validation of Ising-based annealers' output. We demonstrate its behavior through experiments made with actual samples originating from quantum annealer devices.

Keywords

Ising solver, quantum annealing, energy spectrum, quality assessment, cumulants

^{*}kdomino@iitis.pl

[†]koniorczyk.matyas@wigner.hu

1 Introduction

Optimization problems have increasing importance in many fields [1], which is driven by several factors, including the demand for competitiveness, better use of resources, and the increasing complexity and interconnectivity in the contemporary world. However, many problems of practical relevance are computationally hard [2] [3]. Quantum computational devices offer a promising perspective in handling such difficulties [4]. These include quantum annealers, such as the D-Wave machines [5]. In principle, such machines could solve a variety of (hard) optimization problems “naturally” by finding low energy eigenstates encoding the solution [6, 7]. Therefore the development of quantum technology has the potential to efficiently solve complicated (NP-hard in fact [8]) discrete optimization problems by encoding them into the energy of a physical system, thus offering the optimal solution as one of the ground states. Indeed, such a system reaches a state “naturally” via adiabatic evolution [9], from which an optimal solution of the encoded problem can be read out deterministically in principle.

Quantum annealers such as the D-Wave machine are approximate physical realizations of an adiabatic quantum computer, i.e., they are based on a real physical system. They realize a fixed topology of couplings, e.g., Chimera or Pegasus graphs. Thus the optimization problem must be embedded into this topology either as an induced subgraph or in a redundant manner using multiple physical quantum bits to represent a logical one. This procedure is called minor embedding and even though it is often doable relatively simply, finding an optimal embedding is a hard computational problem itself.

No real quantum system can be entirely separated from its environment: the phenomena such as the heat exchange [10] or decoherence [11] cannot be wholly neglected in the case of a physical quantum annealer. This leads to a noisy version of the adiabatic evolution [12]. Moreover, the measurements performed at the last stage of computations are not perfect either. As the dimensionality of the underlying Hilbert space grows exponentially with the number of qubits [13], the aforementioned issues affect the results to an even greater extent. To tackle these problems in a quantum annealing device, the adiabatic evolution is run repeatedly, each run followed by a readout. The results form a statistical sample of configurations and objective values, possibly containing optimal solutions, i.e., the minimum energy states.

The setting of the annealing procedure is challenging, even in the case of an ideal system. The parameters of the process depend on the minimum gap between the instantaneous ground state and the rest of the spectrum during the evolution, which in general, cannot be determined [14]. Therefore, in the observed result, which is the output from a physical quantum annealer, the elements of the output sample can have significantly higher energy than the ground states. Thus, whether any ground state has been sampled, is an important question in practical applications. While in physical applications often it is only the ground state which is useful, in hard optimization problems the low-energy excited states are also valuable. Therefore the question of having states at least close to the ground state in the sample also bears significant relevance.

Reformulation of this question, i.e., the estimation of the success probability of having a ground state in the sample, has also been addressed in the literature of benchmarking, see e.g. [15, 16, 17]. In benchmark scenarios, at least at the present state of the art, the addressed optimization problems are specifically designed, i.e. the ground state is usually known in advance, and the size of a problem is typically small. The success probability is then empirically investigated on the basis of solving various benchmark problems and comparing the result with known solutions. Our idea is different: we propose the complementary method of estimating the *ground-state energy* and testing the quality of the solution against containing any ground state solely using statistical analysis of the output of the Ising machine. We build on certain generic assumptions coming from the statistical description of the system, and therefore our method is more suitable for larger problem instances. This is in line with our intention to use it in application-driven scenarios.

Our goal is to use the entire sample resulting from the use of a quantum annealer (or a similar device) to estimate the likelihood of having a ground state in the sample. We remark here that as quadratic binary optimization problems are NP-hard, bounds on the optimal solution that can be calculated in polynomial time constitute important results in the classical literature of the problem, see e.g., the works of Nesterov [18] or Ye [19]. Those results also provide hints to finding the distance between a particular solution and the optimal one. In a similar spirit, we can consider probabilistic solvers.

In [20] it has been proposed that in future quantum annealer designs, to improve the convergence of solutions into the ground state with the increase of the number of spins, the temperature needs to be scaled down. For high enough temperatures, the cited reference assumes power-law scaling of the heat capacity with temperature. Such scaling is typically a near-phase-transition behavior, similar to the one described by critical exponents. In [20] the relation between the first three cumulants of the Ising energy output and the heat capacity has been calculated using the Boltzmann distribution and the fluctuation-dissipation theorem. We will use this relation to estimate the ground state energy from the spectrum.

Our research is tied to Extreme Value Theory [21] where limits for low values are estimated from a particular probabilistic model of the sample. Instead of estimating the extreme-value distribution, however, we assume its form from the underlying Ising model and use it for estimation of the minimal values.

The paper is organized as follows. In Section 2 a theoretical introduction of our model is presented. In Section 3 the results of our experiments using data both from simulators and real D-Wave machines are discussed. In Section 4 the results are summarized and conclusions are drawn. Appendix A contains more details of performing the Metropolis-Hastings simulations.

2 Theoretical model

Quantum annealers are based on the Ising model defined by the following Hamiltonian:

$$H = \sum_{(i,j) \in \mathcal{E}} J_{i,j} s_i s_j + \sum_{i \in \mathcal{V}} h_i s_i, \quad (1)$$

where \mathcal{V} is a set of spins (vertices), and \mathcal{E} describes the topology of the processor. Let us now briefly recapitulate the considerations in [20], where the energy spectrum of the Ising model was analyzed under the assumption of the Boltzmann distribution, with the techniques of statistical physics. Concerning the effect of finite temperature, the analysis concludes that the probability of sampling the ground state goes to zero exponentially with the number of spins N . The only exception is the case when the ground-state energy H_0 falls into the variation interval of the mean energy. Thus, scaling down the temperature can help in regaining the success probability.

In the considerations of [20] there are two types of scaling of the specific heat with the temperature assumed: power-law for low values of $\beta = \frac{1}{T}$ and exponential for high values (albeit it is claimed as a general assumption that the system is not tuned to a phase transition point). In the present work we focus on the lower range, i.e. relatively high temperatures, as we expect our D-Wave samples to fall into this region. Hence, we will adopt the assumption that specific heat behaves as

$$c(\beta) = -A\beta^{-\alpha-2}, \quad (2)$$

where A is the coefficient of the particular instance, and α is a parameter of the model. From the spread of energies $\sigma(H) = \sqrt{-Nc_\beta}$ from [20], we have:

$$\sigma^2(H) = NA\beta^{-\alpha-2}. \quad (3)$$

Following [20] the mean of the energy distribution of the Ising system can be expressed as:

$$\langle H \rangle = E_0 - N \int_{\beta}^{\infty} c(\beta) d\beta = E_0 + N \frac{A}{\alpha+1} \beta^{-\alpha-1} = E_0 + \frac{\sigma^2(H)\beta}{\alpha+1}, \quad (4)$$

where E_0 is the ground state energy. The asymmetry can be written [20]:

$$\eta(H) = \frac{1}{\sqrt{N}} \frac{1}{(-c(\beta)^{3/2})} \frac{dc(\beta)}{d\beta} = \frac{1}{\sqrt{NA}} (\alpha+2) \beta^{\alpha/2} = \frac{\alpha+2}{\sigma(H)\beta}. \quad (5)$$

Finally, we obtain the formula for the ground state energy, which can be used as an estimator

$$E_0 = \langle H \rangle - \frac{\alpha+2}{\alpha+1} \frac{\sigma(H)}{\eta(H)}. \quad (6)$$

In the similar manner the parameter β can be estimated from data using the following formula

$$\beta = \frac{E_0 - \langle H \rangle}{\sigma(H)\eta(H)(E_0 - \langle H \rangle) - \sigma^2(H)} \quad (7)$$

The ground-state energy and β are thus expressed as a function of cumulants σ , η and $\langle H \rangle$, which will be later estimated from samples.

2.1 Standard error analysis

The output of the quantum annealer (or its simulator) is an n -sample of energies and configurations. Our method uses only the energies as input. The goal is to estimate the ground state energy using methods of moments, i.e., via cumulants computed from the data. Next, we will compare the estimate with the minimum value from the sample in order to assess the likelihood of the event that the sample contains the ground state energy.

To construct the distribution of estimated ground-state energies E_0 in order to obtain a significance threshold, we use Bootstrap resampling [22]. In details, let H_1, H_2, \dots, H_n be a sample, and $E_0(H_1, H_2, \dots, H_n)$ be the estimate of the ground-state energy via Eq. (6). Then from H_1, H_2, \dots, H_n we sample n items with replacements, i.e. repeating some of the elements optionally. Let us denote the resulting samples by $H_1^{(j)}, H_2^{(j)}, \dots, H_n^{(j)}$. For each such sample we compute $E_0^{(j)}$. Repeating this procedure S times we obtain the desired estimated distribution of E_0 -s.

To validate the Bootstrap approach, we compute the standard deviation of E_0 by k -statistics approximation and standard error calculus. In order to do so, it is convenient to use Eq. (6) in the following form:

$$E_0 = \langle H \rangle - \frac{\alpha + 2 \sigma(H)^4}{\alpha + 1} \frac{c_3(H)}{c_3(H)}. \quad (8)$$

Let c_k be the non-normalized k -th order cumulant; we will omit the argument H of all cumulants in what follows. The estimation error of $\langle H \rangle$ can be neglected in comparison to the estimation error of σ^2 and c_3 , as the estimation error of moments (and cumulants) tends to increase with their degree. To estimate the standard deviation of cumulants' estimation, we approximate the cumulants with k -statistics, which is valid for large N [23]. The standard deviation of the cumulants in the argument is:

$$\delta c_3 \approx \sqrt{\frac{c_6 + 9\sigma^2 c_4 + 9c_3^2 + 6\sigma^6}{n}}, \quad (9)$$

and

$$\delta\sigma^2 \approx \sqrt{\frac{c_4 + 2\sigma^4}{n}}. \quad (10)$$

The contributions of the particular cumulants to the standard errors of E_0 are:

$$\delta E_0(c_3) \approx \left| \frac{\partial E_0}{\partial c_3} \right| \delta c_3, \quad \delta E_0(\sigma^2) \approx \left| \frac{\partial E_0}{\partial \sigma^2} \right| \delta \sigma^2. \quad (11)$$

Finally, assuming that estimators are independent, the standard deviation of E_0 can be estimated as

$$\delta E_0 \approx \sqrt{(\delta E_0(c_3))^2 + (\delta E_0(\sigma^2))^2}. \quad (12)$$

2.2 Physical assessment of validity

The results in Ref. [20] serving as the basis of our considerations were obtained by considering and analyzing D-Wave solution for the random instance with couplings $J = \pm 1$ as well as regular 3-regular 3-XORSAT instances and planted (droplet) instances on the Chimera graph. In this context the assumption in Eq. (2) results from the scaling $c_T \sim T^\alpha$ which is appropriate for $\beta \neq \beta_c$ (such a scaling is a phase-transition-like behaviour in β). An actual phase transition would take place in a system of infinite volume, however, as discussed in [24], for finite volume a phase-transition-like behaviour occurs indeed. The larger the system size, the sharper the dependence of c_β on β [25] [26]. We expect a real annealer rather be in the $\beta < \beta_c$ regime as the thermal noise has a significant impact on the machine's output.

Consider a general probabilistic approach to the Ising model with couplings $J_{i,j}$ -s and local fields h_i -s. A phase-transition-like behavior can also be expected under such circumstances, in less rigorous form, though. A simple model of variable coupling can be [27]

$$J_{i,j} = J_0 + \epsilon_{i,j}, \quad (13)$$

where ϵ 's are drawn randomly according to a chosen probability distribution. In [27], it was demonstrated that the presence of such ϵ -s indeed results in a flattening of the exponential scaling. One can claim that for small systems and high variation of couplings, c_β depends weekly on β . Such a phenomenon can possibly affect, for example, the parameter α , making it more instance-dependent in such a case.

Let us also remark that the heat capacity per node depends strongly on the number of connections of the node. In [20] it was assumed that the number of couplings scales linearly with N and also there were additional assumptions on the coupling strength. These do not necessarily hold for our problem instances. As both α and β_c may vary with the degree of connectivity of the graph, the model may behave worse for a problem graph with a highly variable degree of connectivity.

The more detailed analysis of the parameter α will be a subject of further research: a more precise investigation should include the fitting of the α parameter for a particular type of instances and take into consideration α 's estimation error. Here, for demonstration, we will use the $\alpha = 0.19 - 0.38$ parameter already proposed in [20], as well as some lower value of α for wider sensitivity analysis.

3 Experiments

In what follows, we demonstrate the procedure introduced in the previous Section on particular examples. The inputs will be Ising annealer samples, and we shall test whether they contain the ground-state energy.

The described method leads to the following algorithm:

Input:

- Parameter α .
- A sample of energies $\mathbb{H} = (H_1, H_2, \dots, H_n)$ originating from n independent runs of the Ising annealer.

Processing:

- Step 1 (Initialization).
 - Define $H_{\min} = \min(H_1, H_2, \dots, H_n)$;
- Step 2 (Bootstrapping).
Sample with replacements from \mathbb{H} to obtain S Bootstrap samples
$$\mathbb{H}^{(j)} = (H_1^{(j)}, H_2^{(j)}, \dots, H_n^{(j)}),$$
where $j = 1, \dots, S$;
- Step 3 (Estimation of the conditional minimum).
For each $\mathbb{H}^{(j)}$ estimate its minimal value $E_0^{(j)}$ using Eq. (6) with the given value of the parameter α ;
- Step 4 (Estimation of the conditional distribution).
Define a conditional probability measure $\mu^{(\mathbb{H})}$ as an empirical distribution of the data $\{E_0^{(j)}\}_{j=1}^S$;
- Step 5 (Conditional likelihood).
Calculate p -value, i.e.

$$p_{\text{val}} = P_{\mu^{(\mathbb{H})}}(X > H_{\min}) = 1 - P_{\mu^{(\mathbb{H})}}(X \leq H_{\min}),$$

where X is a random variable with the distribution $\mu^{(\mathbb{H})}$;

Output:

- p_{val}

The above procedure provides an estimate of the probability of having a ground state in the sample. A higher value of the parameter also implies probabilistically that at least a lower part of the energy spectrum has been sampled. The estimation in Step 3 assumes the theoretical model from Section 2 and depends on the original sample (\mathbb{H}) and on the result of the draw from Step 2. This estimated probability p_{val} of having sampled a ground state will be referred to as the "p-value" in what follows. The algorithm was implemented in Julia programming language, and the source code is publicly available [28].

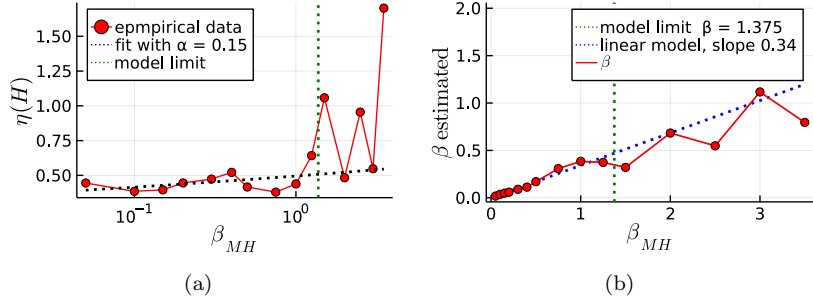


Figure 1: The asymmetry $\eta(H)$ (left) and the estimated β for the artificial data set (right), as a function of the known β_{MH} parameter of the generating Metropolis-Hastings algorithm. In the case of the left part of the figure, the following fitting model was used $\eta \propto \beta_{MH}^{\alpha/2}$. Fitting was performed up to some threshold $\beta_t = 1.375$, termed as the model limit. (This is expected to be instance dependent). The limit was determined by the analysis of the dependence of the β parameter estimated from the sample as the function of the β_{MH} parameter. A linear dependence is expected within model validity, demonstrating that Eq. (7) holds.

3.1 Artificial data

Our first experiments were performed on a problem instance of 198 logical bits from the field of railway operations research, described in detail as a case 1 example in [29], see Section 5.1 therein for a problem description and Section 4.2 for QUBO formulation.

The samples have been generated using the Metropolis-Hastings algorithm. We refer to these data as artificial as they do not come from a physical solver. The Metropolis-Hastings algorithm has β_{MH} as a parameter playing a similar role as the β in our model up to linear scaling in the range of model validity. It is tied to the temperature of the simulated system and thus affects the quality of the solution; the empirical relation of β_{MH} and β , the latter estimated in the way described in Section 3.3. The results of such estimation and the estimated scaling of $\eta(H)$ are presented in Fig. 1. As expected in Section 2.2, we have a limit on β_{MH} , below which scaling in Eq. (5), hence in Eq. (2) holds. To find the threshold, we can analyze the predictive power of the model to determine the temperature of the system via Eq. (7).

In the case of this problem instance, the optimum is known. Hence, we can plot both the difference of the minimum energy state in the sample H_{\min} from the ground state H_0 , and also the p -value as a function of β_{MH} . This is done in Fig. 2. The figure clearly demonstrates that for lower β_{MH} -s, the p -value can be used to distinguish between better and worse solutions. As it will be pointed out later, the actual quantum annealers provide samples with β values that fit in the model validity range.

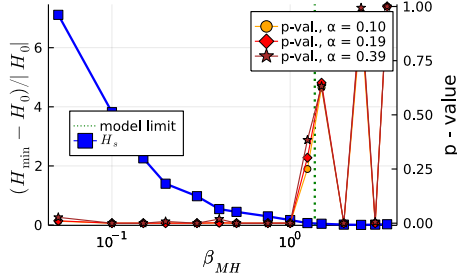


Figure 2: The minimal energy and the p -value for the problem instance addressed in Section 3.1. We have used $S = 1000$ for bootstrapping. In the model validity region (left part limited by the dotted line) $\beta < 1.375$, we can observe 9 true negatives and one solution that is very near the ground state and can be classified as true positive for some threshold of the p -value (such behavior was expected). The choice of the α parameter's values is discussed at the end of Section 2.2. Observe that setting the parameter α to different values does not significantly affect the results. Note also that there was no minor embedding in this case.

To validate the Bootstrap approach, we have compared the standard deviations and the Bootstrap histogram and found them to coincide with those obtained by the direct error calculation in Eq. (12); see Fig. 3.

3.2 Analysis on D-Wave data

We test our algorithm on energy spectra returned by a D-Wave quantum annealer applied either to the set of practical instances or to the set of droplet instances. The first set contains instances from the field of railway operational research [29], see Section 5.1 therein for a more detailed description. The second set contains droplet instances characterized by artificially "planted" ground states [30], designed to be difficult for an annealer. The formulation of droplet instances goes beyond optimization research, such droplet instances are rather designed to benchmark various annealers than to solve any particular problem. Bear in mind that the two types of instances differ in the sense of the variability of couplings and local fields (this issue is important as discussed in Section 2.2). In the case of practical instances, there are many coupling with the same value reflecting a particular set of constraints in the actual problem, which does not hold for the droplet instances.

Data sets are returned by two D-Wave quantum annealers: the D-Wave 2000 (Chimera based); see Figs. 4a, 4b, Tabs. 1a, 1b, Tabs. 2a, 2b and the D-Wave 5000 advantage (Pegasus based); see Fig. 5. In all the experiments, we have used $S = 1000$ for bootstrapping. The relevant parameter here will be the annealing time as it is important to decide whether it was chosen appropriately.

In the case of the practical instances coming from [29] we, therefore, plot

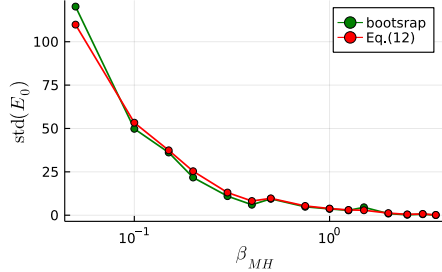
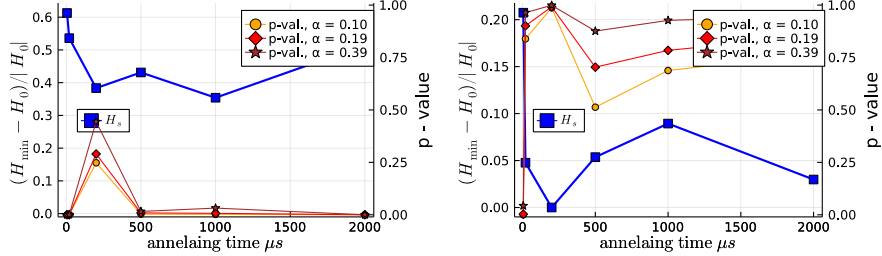


Figure 3: The validation of the Bootstrap approach, the comparison of the standard deviation of the Bootstrap histogram with the E_0 computed via Eq. (6) and standard deviation computed via Eq. (12), $\alpha = 0.19$. Difference between these are small; this has been expected as both bootstrapping and error analysis gave similar standard deviations.

our p -values along with the difference of the energy from the true ground state as a function of the annealing time. This is done in order to demonstrate the usefulness of the p -value in the estimation of whether the right annealing time had been chosen. (We will return to the estimation of the β parameter later.) The corresponding figures: Fig. 4a, Fig. 4b, and Fig. 5 all confirm that the p -value has the expected behavior: it reflects whether the best solution from the sample is close to the ground-state energy. For the set of our practical instances solved on D-Wave, the usefulness of the method has thus been demonstrated; recall that we are interested in low excited states as well. Solutions that are near the ground state (does not differ from ground by more than 10% see Fig. 4b) give high p -values (i.e. above 0.5). Solutions that are further return low p -values.

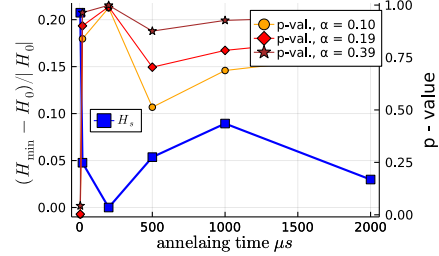
The results for the droplet instances of 2048 physical quantum bits are presented in Tabs. 1a, 1b. The quantum annealer did not succeed in finding the ground state of the larger instances; this is indicated by the p -value. The results for small droplets instances of 128 physical quantum bits are presented in Tabs. 2a, 2b. Here, for short annealing times, some ground states can be detected. (In the case of droplet instances, we are interested only in the ground state, whereas in some other problems, low excited states can also be of interest.). For higher annealing time, the model does not work well; in the case of certain annealing times, the D-Wave output may not obey the Boltzmann distribution). This also supports the observation that our model works better for larger systems.

From the above results, one can see that if the output is far from the ground state (e.g., see worst results on each figure or table), we have almost zero p -value. Hence, a high p -value can be a valid indicator reflecting that the quality of the solution is not very bad. We can consider such procedure as a *primary valuation* of the solution.



(a) 198 logical bits, for highest minimal ener-

gies, the p -value is very low.



(b) 48 logical bits, except from the lowest annealing time, the lowest energies are close to the ground state, which is properly reflected in the p -values.

Figure 4: The p -value validation of the D-Wave solutions of the Chimera practical instances from [29] (Section 5.2 therein). We use the Chimera minor embedding described in details in Section 5.3.3 of [29] with coupling strength $css = 2$. From the pictures, we can conclude that the higher the p -value, the lower the distance between the lowest energy D-Wave sample and the real ground state. Additionally, in the case of Fig. 4a some of solution were evaluated in [29] in the sense of the logistic feasibility, see Fig. 7c therein. p -values coincides with this feasibility, (5 μ s not - feasible, 1000 μ s and 2000 μ s - feasible), our p -value reflects this feasibility.

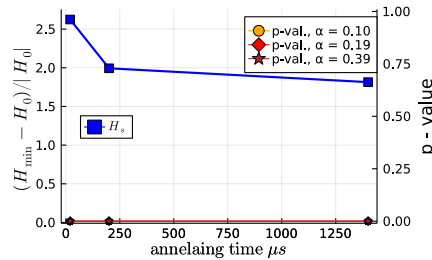


Figure 5: The p -value validation of D-Wave Pegasus instance from [29] with 594 logical bits. We used the Pegasus embedding described in more detail in section 5.4 of [29]. Observe that results were poor; this is reflected in zero p -values.

<i>p</i>-value					$H_{\min} - H_0$				
	it. 1	it. 2	it. 3	it. 4		1	2	3	4
$20\mu\text{s}$	0	0.001	0.005	0.	$20\mu\text{s}$	83	96	102	90
$200\mu\text{s}$	0.024	0	0.001	0.001	$200\mu\text{s}$	64	81	76	61
$2000\mu\text{s}$	0.003	0	0	0.007	$2000\mu\text{s}$	45	67	64	45

(a) *p*-values of particular instances

(b) Difference between the best solution and the ground state energies of approx -3400

Table 1: The *p*-value valuation of solutions for a droplet instance of 2048 physical quantum bits ($\alpha = 0.19$). An item index is an ordinal number. Such instances are designed to be difficult for annealers, and it is reflected in the low *p*-values.

<i>p</i>-value					$H_{\min} - H_0$				
	it. 1	it. 2	it. 3	it. 4		1	2	3	4
$5\mu\text{s}$	0.150	0.0	0.064	0.001	5	0.0	0.24	0.0	1.15
$20\mu\text{s}$	0.256	0.0	0.0	0.001	20	0.0	0.21	0.0	0.0
$200\mu\text{s}$	0.677	0.0	0.0	0.0	200	0.0	0.0	0.0	0.0

(a) *p*-values of particular instances

(b) Difference between the best solution and the ground state energies of approx -210

Table 2: The *p*-value valuation of solutions for a droplet instance of 128 physical quantum bits ($\alpha = 0.19$). An item index is an ordinal number. For short annealing times, there is a potential to detect ground states. For high annealing time, the method does not work properly. Observe the lack of false positives.

3.3 Beta estimation

If the ground state energy is known with certainty (e.g., from some other consideration), we can estimate the β parameter by means of Eq. (7). This parameter reflects the effective temperature of the Ising system realized by the annealer. Therefore it gives information about the extent of noisiness to expect: the lower the β , the closer is the annealer to an ideal adiabatic quantum computer. Meanwhile, as seen in 1, the estimation of β facilitates the comparison with the Metropolis-Hastings approach.

The results are displayed in Tab. 3 (droplet) and Fig. 6 (practical instances). For the studied Chimera instances of practical instances, the β values were found to be higher than those for the Pegasus ones. This suggests that at the time of these calculations, the Pegasus solver was, in a sense, less perfect (noisier) than the Chimera one. For the droplet instances, temperatures are higher; this can be caused either by different scaling of couplings or different working parameters of the physical device. Bear in mind that droplets are complicated instances with highly variable couplings. Hence our model may not work properly for

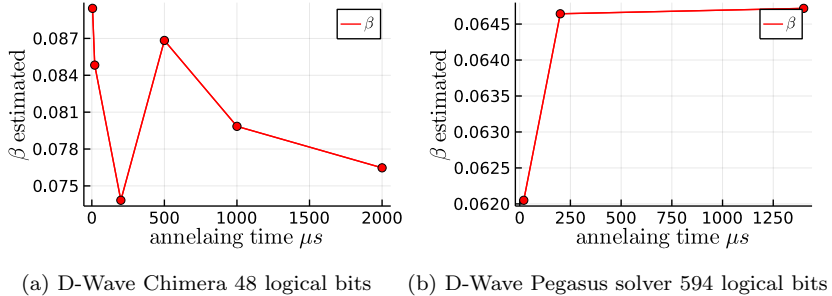


Figure 6: β estimation from practical instances on the Chimera and Pegasus. Observe that the β values are lower for Pegasus, suggesting it is less perfect and more noisy. Here β values are within the model validity.

some smaller droplet instances (where the physical validity of the model may be weaker, see Section 2.2).

β estimated by Eq. (7)				
	it. 1	it. 2	it. 3	it. 4
$20\mu\text{s}$	0.22	0.28	0.37	0.26
$200\mu\text{s}$	0.39	0.31	0.34	0.26
$2000\mu\text{s}$	0.31	0.26	0.27	0.33

Table 3: β estimation from droplet data, 2048 physical quantum bits. Items represents instance ordinal numbers.

4 Conclusions

In this paper, we have introduced an easily implementable method that uses univariate cumulants of order 1 – 3 to assess the quality of the annealer’s output. The method results in a parameter, the p -value, which reflects if the ground state or any excited states close to it have been sampled.

The model depends on the scaling parameter α . We use an ad-hoc value which is plausible according to results in the literature for demonstration. Our sensitivity analysis suggests that the model can be moderately sensitive to α in some cases. Yet, its accurate estimation for the given instance (or set of instances) could improve it. To compute the significance interval, we have applied Bootstrap resampling, a heuristic method. This could also be further improved, e.g., by rescaling the significance interval to fit the variance from the error calculus. We have demonstrated the potential of statistical analysis in the estimation of the quality of Ising annealers’ output on particular examples. At least on the basis of the particular examples of annealer outputs we have studied so far, we

argue that the introduced analysis can serve as a useful tool in the evaluation of the solution. To make a stronger statement, the limitations of our model have to be studied further, both analytically (by elaborating e.g., on the more precise determination of α) and empirically by applying the method to many samples. We plan to use it for additional problems of the field of logistics and operations research, similarly to those e.g., in [31, 32].

As of the possible further steps of this research, recall that in the case of non-Gaussian distributions (like that of the Ising annealer output), information about a probabilistic model can also appear in cumulants of order higher than 3. Hence, applying such cumulants may improve our model. Further, as the annealer output is multivariate (containing energy and spin configurations), the multivariate cumulant analysis can give a further clue in analyzing, qualifying, and perhaps correcting the annealer's output.

Acknowledgments

The research was supported by the Foundation for Polish Science (FNP) under grant number TEAM NET POIR.04.04.00-00-17C1/18-00 (KD, ZP). MK acknowledges the support of the National Research, Development and Innovation Office of Hungary under project numbers K133882 and K124351. This research was supported by the Ministry of Innovation and Technology and the National Research, Development and Innovation Office within the Quantum Information National Laboratory of Hungary.

We would like to thank Bartłomiej Gardas and Łukasz Pawela for valuable tips on physical models and statistical analysis. We thank Özlem Salehi for suggesting valuable references. We thank authors of [30] for supplying the Droplet instances and their D-Wave solutions.

References

- [1] J. Rosenhead, “Reflections on fifty years of operational research,” *Journal of the Operational Research Society*, vol. 60, no. sup1, pp. S5–S15, 2009.
- [2] S. Aaronson, *Quantum Computing Since Democritus*. New York, NY, USA: Cambridge University Press, 2013.
- [3] M. R. Garey and D. S. Johnson, *Computers and intractability*, vol. 174. freeman San Francisco, 1979.
- [4] R. P. Feynman, “There's plenty of room at the bottom,” *Caltech Eng. Sci.*, vol. 23, pp. 22–36, 1960.
- [5] T. Lanting, *et al.*, “Entanglement in a quantum annealing processor,” *Physical Review X*, vol. 4, p. 021041, May 2014.
- [6] Harris, R. *et al.*, “Phase transitions in a programmable quantum spin glass simulator,” *Science*, vol. 361, pp. 162–165, July 2018.

- [7] King, A. at al., “Observation of topological phenomena in a programmable lattice of 1,800 qubits,” *Nature*, vol. 560, pp. 456–460, Aug. 2018.
- [8] A. Lucas, “Ising formulations of many NP problems,” *Frontiers in Physics*, vol. 2, p. 5, 2014.
- [9] E. Farhi, J. Goldstone, S. Gutmann, and M. Sipser, “Quantum computation by adiabatic evolution,” *arXiv preprint quant-ph/0001106*, 2000.
- [10] H. P. Breuer and F. Petruccione, *The Theory of Open Quantum Systems*. Oxford University Press, Oxford, 2002.
- [11] W. H. Zurek, “Decoherence, einselection, and the quantum origins of the classical,” *Reviews of Modern Physics*, vol. 75, pp. 715–775, May 2003.
- [12] L. C. Venuti, T. Albash, D. A. Lidar, and P. Zanardi, “Adiabaticity in open quantum systems,” *Physical Review A*, vol. 93, no. 3, p. 032118, 2016.
- [13] A. Montina, “Exponential complexity and ontological theories of quantum mechanics,” *Physical Review A*, vol. 77, p. 022104, Feb 2008.
- [14] A. M. Childs, E. Farhi, and J. Preskill, “Robustness of adiabatic quantum computation,” *Physical Review A*, vol. 65, p. 012322, Dec. 2001.
- [15] M. Willsch, D. Willsch, F. Jin, H. De Raedt, and K. Michielsen, “Benchmarking the quantum approximate optimization algorithm,” *Quantum Information Processing*, vol. 19, pp. 1–24, 2020.
- [16] D. Willsch, M. Willsch, C. D. G. Calaza, F. Jin, H. De Raedt, M. Svensson, and K. Michielsen, “Benchmarking Advantage and D-Wave 2000Q quantum annealers with exact cover problems,” *arXiv preprint arXiv:2105.02208*, 2021.
- [17] A. S. Koshikawa, M. Ohzeki, T. Kadowaki, and K. Tanaka, “Benchmark test of black-box optimization using d-wave quantum annealer,” *Journal of the Physical Society of Japan*, vol. 90, no. 6, p. 064001, 2021.
- [18] Y. Nesterov, “Semidefinite relaxation and nonconvex quadratic optimization,” *Optimization methods and software*, vol. 9, no. 1-3, pp. 141–160, 1998.
- [19] Y. Ye, “Approximating quadratic programming with bound constraints,” *Mathematical Programming*, vol. 84, pp. 219–226, 1997.
- [20] T. Albash, V. Martin-Mayor, and I. Hen, “Temperature scaling law for quantum annealing optimizers,” *Physical Review Letters*, vol. 119, no. 11, p. 110502, 2017.
- [21] S. Coles, J. Bawa, L. Trenner, and P. Dorazio, *An introduction to statistical modeling of extreme values*, vol. 208. Springer, 2001.

- [22] R. J. Tibshirani and B. Efron, “An introduction to the bootstrap,” *Monographs on statistics and applied probability*, vol. 57, pp. 1–436, 1993.
- [23] E. W. Weisstein, “k-statistic,” <https://mathworld.wolfram.com/>, 2002.
- [24] M. Gligor and M. Ignat, “Econophysics: a new field for statistical physics?,” *Interdisciplinary Science Reviews*, vol. 26, no. 3, pp. 183–190, 2001.
- [25] M. Y. Malsagov, I. Karandashev, and B. Kryzhanovsky, “The analytical expressions for a finite-size 2d ising model,” *arXiv preprint arXiv:1706.02541*, 2017.
- [26] K. Binder, “Overcoming the limitation of finite size in simulations: From the phase transition of the ising model to polymers, spin glasses, etc.,” in *AIP Conference Proceedings*, vol. 690, pp. 74–84, American Institute of Physics, 2003.
- [27] B. Kryzhanovsky, M. Malsagov, and I. Karandashev, “Investigation of finite-size 2D Ising model with a noisy matrix of spin-spin interactions,” *Entropy*, vol. 20, no. 8, p. 585, 2018.
- [28] K. Domino and L. Pawela, “StatisticalVerificationOfIsingEnergies,” 2021. <https://github.com/iitis/StatisticalVerificationOfIsingEnergies>, visited 02.Nov.2021.
- [29] K. Domino, M. Koniorczyk, K. Krawiec, K. Jałowiecki, and B. Gardas, “Quantum computing approach to railway dispatching and conflict management optimization on single-track railway lines,” *arXiv preprint arXiv:2010.08227*, 2020.
- [30] M. M. Rams, M. Mohseni, and B. Gardas, “Heuristic optimization and sampling with tensor networks for quasi-2D spin glass problems,” *arXiv preprint arXiv:1811.06518*, 2019.
- [31] C. Grozea, R. Hans, M. Koch, C. Riehn, and A. Wolf, “Optimising rolling stock planning including maintenance with constraint programming and quantum annealing,” *arXiv preprint arXiv:2109.07212*, 2021.
- [32] Ö. Salehi, A. Glos, and J. A. Miszczak, “Unconstrained binary models of the travelling salesman problem variants for quantum optimization,” *arXiv preprint arXiv:2106.09056*, 2021.
- [33] S. Chib and E. Greenberg, “Understanding the Metropolis-Mastings algorithm,” *The American statistician*, vol. 49, no. 4, pp. 327–335, 1995.

A Metropolis Hastings approach for sampling

One of the presented samples originates from a simulation of an Ising-based annealer with a Metropolis-Hastings approach [33] to sample energy spectrum.

We call these data artificial as they do not come from a physical device. The actual Metropolis-Hastings sampling was performed as follows.

Let \mathbf{s}_k be the configuration of spins at the step k , and let consider its i -th element. Following [33] let $x = \mathbf{s}_k$ be a current solution and y equal to \mathbf{s}_k , but with flip spin at i -th position. Then the probability to move is:

$$\alpha_\beta(x, y) = \begin{cases} \exp(-\beta_{\text{MH}}(H(y) - H(x))) & \text{if } H(y) \geq H(x) \\ 1 & \text{if } H(y) < H(x), \end{cases} \quad (14)$$

where the Gibbs distribution with β_{MH} parameter is used. If β_{MH} is low ,jumps to “better” solutions are favorable, while if the beta is large, the more extensive search of the solution space is favorable.